JOURNAL OF GEOPHYSICAL RESEARCH, VOL. 106, NO. D5, PAGES 4815–4829, MARCH 16, 2001

A parameterization of an aerosol physical chemistry model for the $NH_3/H_2SO_4/HNO_3/H_2O$ system at cold temperatures

Jin-Sheng Lin

Bay Area Environmental Research Institute, San Francisco, California

Azadeh Tabazadeh

NASA Ames Research Center, Moffett Field, California

Abstract. Simple expressions are fitted to the results obtained from ion interaction thermodynamic models for calculating HNO_3 and H_2O vapor pressures over the $NH_3/H_2SO_4/HNO_3/H_2O$ system at cold temperatures. The vapor pressure expressions are incorporated into a mass conserving equilibrium solver for computing aerosol compositions in the lower stratosphere and upper troposphere. The compositions calculated from the aerosol physical chemistry model (APCM) are compared against previous parameterizations. The APCM compositions are in better agreement with the compositions obtained from ion interaction models than from other previous formulations of the $NH_3/H_2SO_4/HNO_3/H_2O$ system. The only advantage of the APCM over the ion interaction approach is that the numerical scheme used in the model is fast and efficient for incorporation into large-scale models. The APCM is used to calculate HNO_3 solubility in ammoniated aerosols as a function of HNO_3, H_2SO_4 and NH_3 mass loadings in the lower stratosphere and upper troposphere. While the uptake of HNO_3 by ammoniated aerosols is strongly dependent upon the solution neutrality (or pH), we find that in both the lower stratosphere and upper troposphere a significant fraction of HNO_3 will exist in aerosol solutions near and below the ice frost point irrespective of solution neutrality.

1. Introduction

Thermodynamic electrolyte models are often used for calculating properties of inorganic aerosols in the lower troposphere [*Stelson and Seinfeld*, 1981; *Pilinis and Seinfeld*, 1987; *Wexler and Seinfeld*, 1991; *Kim and Seinfeld*, 1995; *Jacobson et al.*, 1996; *Jacobson*, 1999b] and stratosphere [*Tabazadeh et al.*, 1994; *Carslaw et al.*, 1994, 1995b; *Weisenstein et al.*, 1997]. In the lower troposphere, aerosol models are often used in air quality studies to assess the effects of aerosols on health, gas-phase partitioning, and visibility. In the stratosphere, aerosol models have been used to simulate the formation and growth of polar stratospheric clouds, which are linked to stratospheric ozone depletion [*Solomon*, 1999]. However, thermodynamic treatments in large-scale atmospheric models are in general not suited for calculating aerosol compositions in the upper troposphere. Since upper tropospheric aerosols participate in the nucleation and growth of cirrus clouds and may also be involved in the scavenging of trace gas species, it is important to understand their chemical and physical properties [*Kärcher and Solomon*, 1999].

Recently, equilibrium aerosol formulations have been incorporated into three-dimensional models to simulate the radiative impacts of aerosols on climate [*Adams et al.*, 1999; *Jacobson*, 2000]. In this work, an aerosol physical chemistry model (APCM) with an efficient solving scheme suitable for incorporation into large-scale atmospheric models is developed. The APCM is compared against various parameterizations, including results from the aerosol inorganics model (AIM2) of *Clegg et al.* [1998a].

Paper number 2000JD900598.
0148-0227/01/2000JD900598$09.00

2. Background on Thermodynamic Aerosol Models

2.1. Ion Interaction Approach

The ion interaction approach is originally based on the work of *Pitzer* [1991]. The solution behavior in Pitzer's method is determined by a series of single-ion (and water) activity equations that are based on

Table 1. A_n Coefficients for the Vapor Pressure of HNO_3[a]

r	a_0	a_1	a_2	a_3	a_4	a_5	a_6	a_7
0.0	12.6923	-0.0325979	-0.071719	0.812331	2.34482	0.000438486	-0.00428908	-0.000709075
0.1	12.4691	-0.0019955	-0.077484	0.727085	2.42858	0.000259723	-0.00442994	-0.000706633
0.2	12.2326	0.0260933	-0.085355	0.644593	2.52519	9.32848e-05	-0.00453571	-0.000694942
0.3	11.9840	0.0513596	-0.094561	0.567113	2.63058	-5.53402e-05	-0.00461276	-0.000678339
0.4	11.7205	0.0725417	-0.104727	0.500403	2.74278	-0.000172282	-0.00466394	-0.000659102
0.5	11.4289	0.0880553	-0.116820	0.450799	2.86783	-0.000241534	-0.00468708	-0.000632214
0.6	11.0837	0.0983196	-0.134271	0.415462	3.02666	-0.000267273	-0.00467490	-0.000579027
0.7	10.6697	0.106923	-0.160517	0.378195	3.24022	-0.000284624	-0.00461980	-0.000480710
0.8	10.2087	0.117295	-0.194708	0.324242	3.50279	-0.000327867	-0.00451884	-0.000342092
0.9	9.73753	0.130202	-0.232997	0.251054	3.79040	-0.000406493	-0.00437409	-0.000184569
1.0	9.28445	0.144365	-0.271608	0.165018	4.07962	-0.000510598	-0.00418932	-2.90206e-05
1.1	8.87335	0.156600	-0.306440	0.080649	4.34517	-0.000611458	-0.00396949	0.000101871
1.2	8.55964	0.157392	-0.327751	0.039034	4.52665	-0.000618013	-0.00372273	0.000153819
1.3	8.33474	0.134427	-0.331971	0.092212	4.60197	-0.000411043	-0.00345255	0.000106943
1.4	7.95881	0.110127	-0.354342	0.142888	4.78919	-0.000208202	-0.00313268	0.000158658
1.5	7.51749	0.0956133	-0.390173	0.143658	5.05815	-0.000120908	-0.00275735	0.000282545
1.6	7.14929	0.0860305	-0.421553	0.118501	5.29796	-0.000104343	-0.00234767	0.000379673
1.7	6.88502	0.0761817	-0.441786	0.092775	5.46818	-0.000107787	-0.00192436	0.000413991
1.8	6.68262	0.0630763	-0.453078	0.080818	5.58436	-0.000101314	-0.00149773	0.000397780
1.9	6.43124	0.0455338	-0.465952	0.086457	5.71507	-7.48198e-05	-0.00106043	0.000386668
2.0	5.72588	0.0242624	-0.524014	0.096528	6.13955	-5.31470e-05	-0.00053951	0.000609824
∞[b]	11.5869	0.222271	-0.109389	0.279027	2.83237	-0.00101574	-0.00488557	-0.000704950

[a] $A_n = a_0 + a_1 w_1 + a_2 w_2 + a_3\sqrt{w_1} + a_4\sqrt{w_2} + a_5 w_1^2 + a_6 w_1 w_2 + a_7 w_2^2$.

[b] The ∞ represents the ternary system of $NH_3/HNO_3/H_2O$ (i.e., $H_2SO_4 = 0$).

thermodynamic properties of mixed solutions. Physical parameters for the fundamental activity relations in an ion interaction model are fitted to laboratory measurements of solute-water mixtures of interest. Thermodynamic electrolyte models based on the ion interaction approach have evolved significantly in recent years by Clegg and coworkers [e.g., *Clegg and Brimblecombe*, 1990, 1995a, 1995b; *Carslaw et al.*, 1995a; *Clegg et al.*, 1998a, 1998b]. Since the models of Clegg and coworkers, collectively referred to as aerosol inorganics model (AIM2), are fitted to laboratory measurements conducted over a broad temperature range (< 200 to 328°K), they are more accurate than those based on the common binary activity approach described in section 2.2. However, the complex nature of the ion interaction approach makes AIM2 computationally impractical for three-dimensional applications. Here we use AIM2 to generate solution compositions and vapor pressures for the $NH_3/H_2SO_4/HNO_3/H_2O$ system for a wide range of humidities and temperatures.

2.2. Binary Activity Approach

The second approach first emerged from modeling inorganic aerosols in air quality studies [e.g., *Stelson and Seinfeld*, 1981; *Bassett and Seinfeld*, 1983; *Saxena et al.*, 1986]. This method separates out water (via either the Gibbs-Duhem equation or the water equation [*Stokes and Robinson*, 1966]) and solute activity coefficients. Usually, a mixing rule of either *Bromley* [1973] or *Kusik and Meissner* [1978] is used to estimate the mixed solute activity coefficients. The equilibrium models based on this approach require only a knowledge of water and solute activity coefficients at a binary level. Thermodynamic models based on the binary activity approach are computationally more efficient but less accurate than the ion interaction approach because the physics of the activity coefficients in the former approach are mainly based on the behavior of binary solutions instead of mixed solution properties used in the latter formulations. To contrast two different thermodynamic treatments, we will update an equilibrium model based on the binary activity approach, EQUISOLV II [*Jacobson et al.*, 1996; *Jacobson*, 1999b], and compare its predictions against results obtained from AIM2. EQUISOLV II applies a well-converged numerical solver scheme to simultaneously solve a large number of equilibrium equations.

2.3. Vapor Pressure Approach

A combination of the two approaches outlined in sections 2.1 and 2.2 is used in this work to develop a fast and accurate parameterization of the $NH_3/H_2SO_4/$

Table 2. B_n Coefficients for the Vapor Pressure of HNO_3[a]

r	b_0	b_1	b_2	b_3	b_4	b_5	b_6	b_7
0.0	-7672.46	67.7280	32.3655	-259.196	-235.30	-0.256884	0.97336	0.197376
0.1	-7609.77	50.7068	32.9809	-222.190	-255.43	-0.131368	1.07699	0.201805
0.2	-7541.22	35.7444	34.4801	-189.780	-280.54	-0.026085	1.16451	0.202182
0.3	-7467.24	22.7871	36.6718	-162.151	-309.62	0.059118	1.23812	0.199536
0.4	-7387.11	11.9765	39.4988	-140.155	-342.40	0.122744	1.29896	0.194190
0.5	-7297.89	3.4748	43.2297	-124.533	-380.56	0.163341	1.34688	0.184702
0.6	-7194.29	-3.0516	48.6478	-113.773	-428.87	0.184446	1.38064	0.166777
0.7	-7074.27	-8.6193	56.4190	-103.509	-491.39	0.196255	1.39907	0.136740
0.8	-6944.62	-14.0870	66.1301	-90.235	-565.46	0.207582	1.40222	0.096867
0.9	-6815.18	-19.5849	76.6808	-73.739	-644.27	0.220387	1.39134	0.053245
1.0	-6693.25	-24.6807	87.0206	-56.230	-721.33	0.231211	1.36800	0.011651
1.1	-6584.97	-28.3719	96.0022	-42.304	-789.58	0.230911	1.33398	-0.021582
1.2	-6504.53	-27.8717	100.995	-44.004	-832.71	0.192747	1.29170	-0.031795
1.3	-6449.42	-19.3426	100.908	-77.488	-843.95	0.079582	1.24188	-0.012861
1.4	-6347.58	-8.4904	106.038	-117.723	-886.93	-0.052980	1.17584	-0.022354
1.5	-6203.79	-0.1957	118.040	-143.506	-971.43	-0.156090	1.08786	-0.069346
1.6	-6055.69	4.8272	133.047	-152.440	-1073.17	-0.221191	0.98027	-0.132468
1.7	-5927.18	6.8545	148.101	-146.787	-1173.72	-0.249961	0.85834	-0.195765
1.8	-5829.77	6.2290	161.504	-129.145	-1262.57	-0.245338	0.72779	-0.250386
1.9	-5768.38	3.1411	172.326	-101.381	-1334.05	-0.209351	0.59425	-0.291726
2.0	-5744.66	-2.5250	180.115	-63.965	-1385.49	-0.141562	0.46318	-0.317848
∞[b]	-7298.14	-51.7642	35.6176	-55.070	-360.093	0.376735	1.41665	0.252861

[a] $B_n = b_0 + b_1 w_1 + b_2 w_2 + b_3\sqrt{w_1} + b_4\sqrt{w_2} + b_5 w_1^2 + b_6 w_1 w_2 + b_7 w_2^2$.

[b] The ∞ represents the ternary system of $NH_3/HNO_3/H_2O$ (i.e., $H_2SO_4 = 0$).

HNO_3/H_2O system for atmospheric applications. The vapor pressure approach requires generation of large sets of H_2O and HNO_3 vapor pressure arrays over the $NH_3/H_2SO_4/$ HNO_3/H_2O system for many assumed compositions and temperatures. The vapor pressure, composition, and temperature fields generated are fitted into simple mathematical expressions similar to those derived by *Luo et al.* [1995] for the $H_2SO_4/HNO_3/H_2O$ system. The vapor pressure relations are then inserted into a numerical mass-conserving equilibrium solver similar to that used in EQUISOLV II [*Jacobson et al.*, 1996] for gas-aerosol phase partitioning calculations.

3. Model Development

3.1. Aerosol Physical Chemistry Model (APCM)

Luo et al. [1995] have shown that equilibrium partial pressures of HNO_3 and H_2O over the $H_2SO_4/HNO_3/H_2O$ system roughly follow a Clausius-Clapeyron relation of the form $\ln P = A + B/T$ (where P is pressure, T is temperature, and A and B are constants) for a fixed solution composition. For the quaternary system of $NH_3/H_2SO_4/HNO_3/H_2O$ we found a similar behavior for the variation of HNO_3 and H_2O vapor pressures over the solution.

Assuming that NH_3 and H_2SO_4 reside completely in the condensed phase (i.e., both $NH_{3(g)}$ and $H_2SO_{4(g)}$ are negligible), we follow the approach of *Luo et al.* [1995] and define w_1 and w_2 as the weight percents of ammoniated sulfate and nitric acid, respectively, in the solution as follows:

$$w_1 = \text{weight \% of } (NH_4)_r H_{2-r} SO_{4(aq)},$$

$$w_2 = \text{weight \% of } HNO_{3(aq)}, \quad (1)$$

$$r = \frac{NH_3}{H_2SO_4} = \frac{NH^+_{4(aq)}}{HSO^-_{4(aq)} + SO^{2-}_{4(aq)}}, \quad (2)$$

where r in w_1 is the fixed mole ratio of ammonia to sulfuric acid, and (aq) is the aqueous-phase species. The r ratio can be considered as the degree of the ammoniated solution neutrality and can take on any values in APCM (including fractions) between 0.0 and 2.0. For example, if r equals 0.0, 1.0, and 2.0, w_1 represents the weight percents of H_2SO_4, $(NH_4)HSO_4$, and $(NH_4)_2SO_4$, respectively, in the solution. Using *Clegg et al.*'s [1998a] model, we first generated a series of arrays of HNO_3 and H_2O vapor pressures for a wide range of weight percent

Table 3. C_w Coefficients for the Vapor Pressure of H_2O[a]

r	c_0	c_1	c_2	c_3	c_4	c_5	c_6	c_7
0.0	22.7490	0.0424817	0.0533280	-0.0567432	-0.276555	-0.000621533	-0.000311769	-0.000283120
0.1	22.7669	0.0310031	0.0493720	-0.0270045	-0.265333	-0.000496930	-0.000261912	-0.000257919
0.2	22.7838	0.0223810	0.0457014	-0.0059721	-0.254223	-0.000403349	-0.000224673	-0.000234421
0.3	22.8005	0.0165207	0.0423183	0.0065020	-0.243407	-0.000339520	-0.000198990	-0.000212594
0.4	22.8179	0.0132215	0.0393297	0.0110504	-0.233647	-0.000303073	-0.000184277	-0.000192973
0.5	22.8367	0.0119853	0.0369883	0.0096303	-0.226435	-0.000288721	-0.000180339	-0.000177085
0.6	22.8556	0.0119008	0.0354244	0.0058633	-0.222617	-0.000287316	-0.000186497	-0.000165709
0.7	22.8706	0.0122336	0.0342757	0.0024714	-0.220187	-0.000291401	-0.000201103	-0.000156776
0.8	22.8791	0.0129460	0.0329580	-0.0009337	-0.215893	-0.000300122	-0.000221710	-0.000146949
0.9	22.8818	0.0143893	0.0311831	-0.0063234	-0.208231	-0.000316451	-0.000246179	-0.000134615
1.0	22.8812	0.0168828	0.0289977	-0.0153842	-0.197574	-0.000343217	-0.000273061	-0.000120122
1.1	22.8803	0.0204917	0.0267376	-0.0284821	-0.185921	-0.000381016	-0.000302055	-0.000105483
1.2	22.8846	0.0243030	0.0255578	-0.0417119	-0.179964	-0.000421023	-0.000333949	-9.75631e-05
1.3	22.8946	0.0259818	0.0267000	-0.0449953	-0.186824	-0.000440711	-0.000370519	-0.000103697
1.4	22.8950	0.0265182	0.0275800	-0.0428170	-0.191549	-0.000449334	-0.000409584	-0.000108446
1.5	22.8866	0.0275456	0.0272887	-0.0426774	-0.189011	-0.000462731	-0.000447757	-0.000106656
1.6	22.8752	0.0293967	0.0263037	-0.0461528	-0.182140	-0.000484748	-0.000483688	-0.000101242
1.7	22.8640	0.0319034	0.0251308	-0.0524783	-0.173920	-0.000514332	-0.000517346	-9.51958e-05
1.8	22.8542	0.0347733	0.0240901	-0.0603014	-0.166228	-0.000549028	-0.000549196	-9.03611e-05
1.9	22.8459	0.0376949	0.0233346	-0.0682171	-0.159987	-0.000586063	-0.000579624	-8.75512e-05
2.0	22.8381	0.0403666	0.0228641	-0.0749269	-0.155242	-0.000622692	-0.000608700	-8.66960e-05
∞[b]	22.7279	0.0163541	0.0303799	-0.0208336	-0.151376	-0.000354967	-0.000653371	-0.000197299

[a] $C_w = c_0 + c_1 w_1 + c_2 w_2 + c_3\sqrt{w_1} + c_4\sqrt{w_2} + c_5 w_1^2 + c_6 w_1 w_2 + c_7 w_2^2$.

[b] The ∞ represents the ternary system of $NH_3/HNO_3/H_2O$ (i.e., $H_2SO_4 = 0$).

combinations (w_1, w_2; where $0.0\% \le w_1 + w_2 \le 85.0\%$) at cold temperatures, ranging from 180 to 270°K. The vapor pressures were then fitted into the following functions:

$$0.0\% \le w_1 + w_2 \le 85.0\%, \quad 180^\circ K \le T \le 270^\circ K, \quad (3)$$

$$\ln P_{HNO_3} = A_n(r, w_1, w_2) + \frac{B_n(r, w_1, w_2)}{T}, \quad (4)$$

$$\ln P_{H_2O} = C_w(r, w_1, w_2) + \frac{D_w(r, w_1, w_2)}{T}, \quad (5)$$

where P_{HNO_3} and P_{H_2O} are in mbar. Coefficients A_n, B_n, C_w, and D_w were then parameterized into a mathematical function of w_1 and w_2 similar to that described by *Luo et al.* [1995]. The fitting results are summarized in Tables 1-4 for different r ratios, ranging from 0.0 and 2.0 (r values are separated by an increment of 0.1).

In Plate 1 the calculated vapor pressures using equations (4) and (5) are compared with those obtained from AIM2 for three r ratios (shown in Plates 1a, 1b, and 1c). In general, P_{H_2O} calculated by equation (5) agrees well with the model of *Clegg et al.* [1998a]. However, the agreement of P_{HNO_3} using equation (4) is rather poor for most compositions. As shown in Plate 1, the calculated P_{HNO_3} becomes increasingly inaccurate as the solution neutrality (i.e., r) increases. For some cases the difference between estimated P_{HNO_3} values and those predicted by AIM2 reached as high as a factor of 5. To ensure differences are minimized, Diff terms accounting for the differences (deviations) of the "calculated" values (estimated from equations (4) and (5)) and the "real" values (obtained from AIM2) were added to equations (4) and (5):

$$\ln P_{HNO_3} = A_n(r, w_1, w_2) + \frac{B_n(r, w_1, w_2)}{T} + \mathrm{Diff}_n(r, w_1, w_2, T) \quad (6)$$

$$\ln P_{H_2O} = C_w(r, w_1, w_2) + \frac{D_w(r, w_1, w_2)}{T} + \mathrm{Diff}_w(r, w_1, w_2, T). \quad (7)$$

For a fixed r, w_1, and w_2 the Diff correction terms approximately follow simple polynomial functions in temperature:

$$\mathrm{Diff}_n(r, w_1, w_2, T) = \sigma_{n0} + \sigma_{n1} T + \sigma_{n2} T^2 \quad (8)$$

Table 4. D_w Coefficients for the Vapor Pressure of H_2O[a]

r	d_0	d_1	d_2	d_3	d_4	d_5	d_6	d_7
0.0	-5850.24	21.9744	1.48745	-44.5210	59.6400	-0.384362	-0.644671	-0.208556
0.1	-5849.94	19.8594	1.73322	-39.7129	58.0581	-0.336545	-0.606959	-0.210361
0.2	-5849.15	17.5776	1.92716	-34.3704	56.5456	-0.289409	-0.568784	-0.211815
0.3	-5848.04	15.1511	2.06677	-28.5548	55.1548	-0.243024	-0.530295	-0.212915
0.4	-5846.79	12.6262	2.12829	-22.4377	54.0535	-0.197733	-0.491539	-0.213544
0.5	-5845.48	10.1120	2.06175	-16.4657	53.5369	-0.154503	-0.452501	-0.213397
0.6	-5843.72	7.79449	1.85460	-11.3889	53.6970	-0.115030	-0.413300	-0.212396
0.7	-5840.63	5.79437	1.60810	-7.6468	53.9687	-0.0803938	-0.374279	-0.211123
0.8	-5835.71	4.05810	1.46205	-4.9098	53.5707	-0.0500282	-0.335935	-0.210378
0.9	-5829.33	2.44674	1.47151	-2.5108	52.2170	-0.0225318	-0.298645	-0.210471
1.0	-5822.28	0.84270	1.60302	0.0831	50.1179	0.0033213	-0.262577	-0.211194
1.1	-5815.44	-0.79036	1.74377	2.9989	47.9281	0.0280087	-0.227587	-0.211883
1.2	-5810.31	-2.20859	1.55496	5.1396	47.5949	0.0492844	-0.193207	-0.210535
1.3	-5807.19	-2.71615	0.62592	3.4557	51.4599	0.0605252	-0.158668	-0.204729
1.4	-5801.66	-2.43122	-0.39261	-1.5150	55.7388	0.0628630	-0.124306	-0.198357
1.5	-5792.68	-1.85557	-1.06065	-7.4818	57.9126	0.0612095	-0.091134	-0.193964
1.6	-5781.23	-1.28487	-1.31402	-13.0971	57.6578	0.0586697	-0.059876	-0.191880
1.7	-5768.33	-0.88563	-1.18923	-17.6257	55.2142	0.0571507	-0.030919	-0.191856
1.8	-5754.83	-0.75269	-0.74364	-20.6765	50.9331	0.0578653	-0.004421	-0.193536
1.9	-5741.30	-0.93290	-0.03072	-22.0791	45.1436	0.0615518	0.019549	-0.196612
2.0	-5728.09	-1.44363	0.91523	-21.7913	38.0640	0.0686466	0.040959	-0.200889
∞[b]	-5736.70	-0.27462	2.02241	0.5073	20.6699	0.0337051	-0.045872	-0.179320

[a] $D_w = d_0 + d_1 w_1 + d_2 w_2 + d_3\sqrt{w_1} + d_4\sqrt{w_2} + d_5 w_1^2 + d_6 w_1 w_2 + d_7 w_2^2$.

[b] The ∞ represents the ternary system of $NH_3/HNO_3/H_2O$ (i.e., $H_2SO_4 = 0$).

$$\mathrm{Diff_w}(r, w_1, w_2, T) = \sigma_{w0} + \sigma_{w1} T + \sigma_{w2} T^2, \quad (9)$$

where σ are second order polynomial coefficients fitted for a particular combination of w_1, w_2, and r. The effects of including Diff terms in improving the vapor pressure fits are shown in Plates 1d-1f where HNO_3 and H_2O vapor pressures calculated from equations (6) and (7) (with polynomial coefficients of equations (8) and (9)) are compared against AIM2 results for the same r ratios examined above. As shown in Plates 1d-1f, Diff terms force the calculated vapor pressures of both H_2O and HNO_3 to agree with AIM2 results. For r values other than 0.0, 1.0, and 2.0, including Diff terms in vapor pressure relations produces a nearly exact agreement with AIM2 results. Thus, for APCM we tabulated polynomial coefficients of σ (lookup tables available as electronic supporting material[1]) for all possible combinations of w_1, w_2, and r. The weight percents of w_1 and w_2 in the lookup tables cover and span the composition spectrum from 0.0% to 85.0% with 1% increments in composition.

As temperatures cool, solubilities of trace gases, such as nitric acid, increase significantly, thereby depleting gas phase concentrations. Thus it is essential to calculate the distribution of HNO_3 between the gas and aerosol phases. To simulate the gas–aerosol partitioning of HNO_3, equations (6) and (7) are coupled with mass conservation of HNO_3:

$$\text{total } HNO_3 = P_{HNO_3} + HNO_{3(aq)} \quad (\text{in mol/m}^3). \quad (10)$$

Three unknowns, $(NH_4)_r H_{2-r} SO_{4(aq)}$ (or w_1), $HNO_{3(aq)}$ (or w_2), and P_{HNO_3}, can be uniquely determined by equations (6), (7), and (10). For this work, the same numerical scheme as that utilized in EQUISOLV II [*Jacobson et al.*, 1996] is applied to solve equations (6)-(10) iteratively.

At iteration steps where w_1 and w_2 are not tabulated in the lookup tables, the bilinear (area weighted) averaging [*Jacobson*, 1999a] is adopted for interpolation. For example, to estimate properties at $[w_1, w_2] = [25.3, 10.8]$, results obtained from four adjacent points,

[1]Supporting lookup tables are available via Web browser or via Anonymous FTP from ftp://kosmos.agu.org, directory "apend" (Username = "anonymous", Password = "guest"); subdirectories in the ftp site are arranged by paper number. Information on searching and submitting electronic supplements is found at http://www.agu.org/pubs/esupp_about.html.

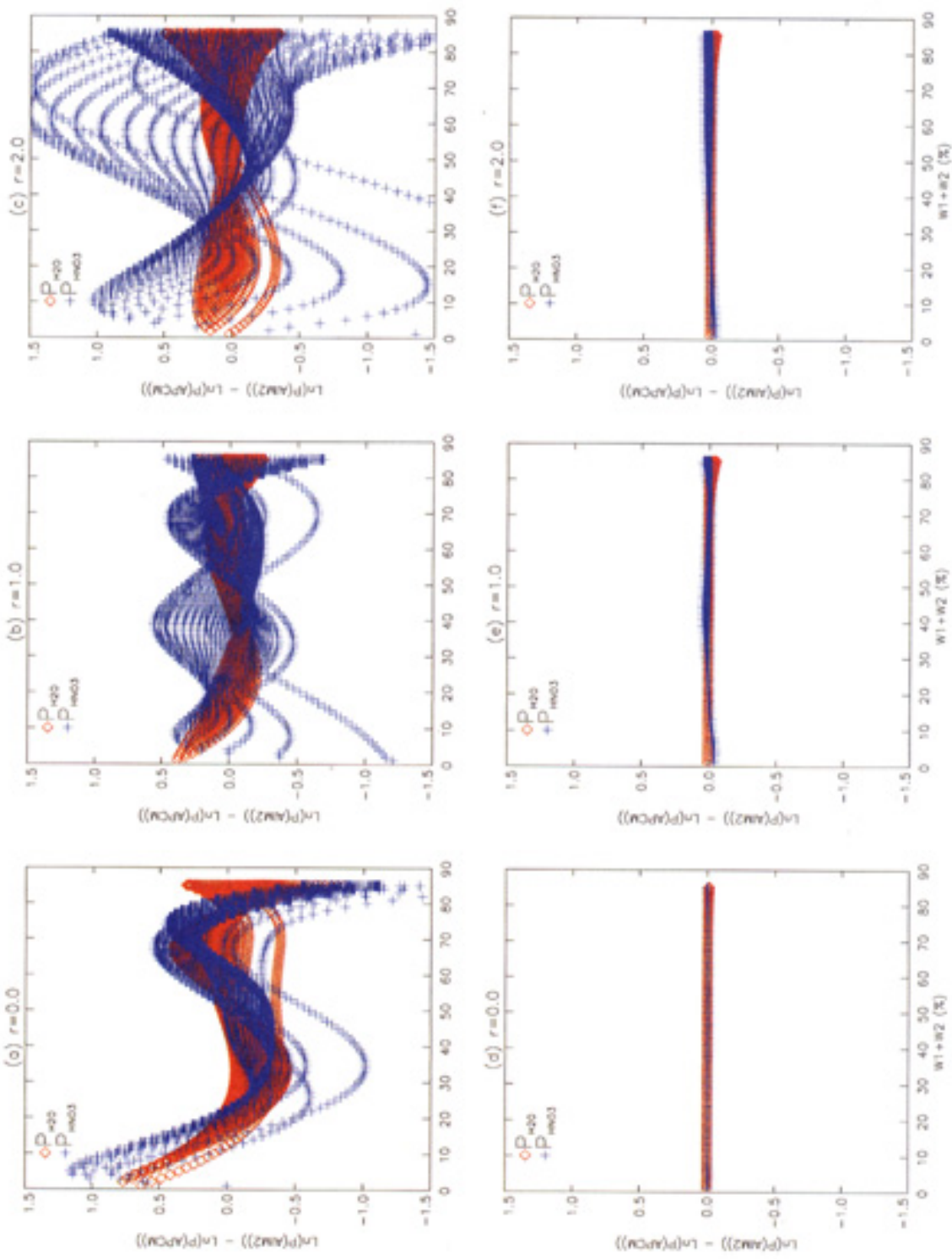

Plate 1. Comparison of vapor pressures obtained from APCM parameterization and those predicted by AIM2 for three r ratios. (a, b, c) Vapor pressures calculated by equations (4) and (5), and (d, e, f) results calculated by equations (6) and (7).

Table 5. Composition Functions[a]

	A	B	C	D
		$(NH_4)_2SO_4$		
$0.00 < a_w < 0.30$				
y_1	5.1229560233e+01	−9.6193408336e−01	1.4720578701e+02	−1.7229112367e−02
y_2	4.5462384945e+01	−9.4872028917e−01	3.3412155166e+02	−2.1124614825e+02
$0.30 \leq a_w < 0.60$				
y_1	9.7348916855e−01	−2.7444251275e+00	−1.8966528614e+01	1.9212056647e+01
y_2	1.0148647694e+00	−2.3916961554e+00	−2.2987950986e+01	2.1920018865e+01
$0.60 \leq a_w \leq 1.00$				
y_1	−5.3756389490e+02	1.3556456453e−02	−1.8951248281e+01	5.5692105238e+02
y_2	−4.2921431877e+02	1.2875856340e−02	−2.1275933520e+01	4.5075478762e+02
		NH_4NO_3		
$0.00 < a_w < 0.40$				
y_1	1.3165236133e+02	−1.0103415600e+00	−3.1726829968e+01	−1.4042075761e+02
y_2	8.1149051028e+01	−9.6213385243e−01	1.0536766694e+02	−1.5360919227e+02
$0.40 \leq a_w < 0.85$				
y_1	8.5782004669e+01	−1.2795635979e+00	2.9982661442e+01	−1.0776290885e+02
y_2	3.2723371194e+01	−1.3299217851e+00	−8.1245973075e+00	−2.4520261799e+01
$0.85 \leq a_w \leq 1.00$				
y_1	−1.4969599516e−01	−2.0271382540e+01	−2.1065828892e+02	2.0679076661e+02
y_2	1.6636062187e+03	−1.3465428608e−01	1.8592287444e+02	−1.8496676635e+03
		NH_4HSO_4		
$0.00 < a_w < 0.25$				
y_1	8.9148556445e+01	−9.2225449765e−01	2.1668157712e+02	−2.7552338531e+02
y_2	5.9840874514e+01	−9.3729948048e−01	2.7226224522e+02	−2.1721584622e+02
$0.25 \leq a_w < 0.80$				
y_1	2.8756459725e+00	−2.5507156109e+00	−3.3316860933e−01	−1.8494214012e−03
y_2	3.5550024880e+00	−2.0910350500e+00	−1.0492539829e+01	7.8923013513e+00
$0.80 \leq a_w \leq 1.00$				
y_1	−1.4227339985e+00	2.9277231432e+01	−1.7215058088e+01	1.8441662636e+01
y_2	−7.0483234774e−01	2.0832745270e+01	−2.3289593929e+01	2.3901137559e+01

[a] $y = Aa_w^B + Ca_w + D$. Read 5.1229560233e+01 as 5.1229560233×10^1. All parameterizations are valid for 190^o K $\leq$ T $\leq$ 260^o K only. Molality m is calculated by $m(a_w, T) = y_1(a_w) + (T - 190)[y_2(a_w) - y_1(a_w)]/70$, where a_w is water activity (relative humidity expressed in fraction). Composition functions for H_2SO_4 and HNO_3 in the same mathematical form are given by *Tabazadeh et al.* [1997a, 1997b].

[25.0, 10.0], [25.0, 11.0], [26.0, 10.0], [26.0, 11.0], are weighted and averaged, depending on how far the desired point is located away from the four fixed points. Similarly, a simple linear interpolation (of averaging predictions from two adjacent r ratios) is implemented if initial r falls inbetween the 0.1 increments (see Table 1). Since the intervals are small (1% for w_1 and w_2 and 0.1 for r), the two interpolation methods yield reasonable results that are in close agreement with AIM2 in predicting HNO_3 and H_2O vapor pressures over the $NH_3/H_2SO_4/HNO_3/H_2O$ system.

For conditions where H_2SO_4 mixing ratio is zero we define w_1 and w_2 as the weight percents of $NH_4NO_{3(aq)}$ and $HNO_{3(aq)}$, respectively, and repeat the above steps to obtain vapor pressures and solution compositions for the $NH_3/HNO_3/H_2O$ system.

3.2. An Update of EQUISOLV II

In addition to APCM parameterization an equilibrium model based on the binary activity approach [*Stelson and Seinfeld*, 1981; *Pilinis and Seinfeld*, 1987; *Wexler and Seinfeld*, 1991; *Kim and Seinfeld*, 1995; *Jacobson et al.*, 1996; *Jacobson*, 1999b], EQUISOLV II [*Jacobson et al.*, 1996; *Jacobson*, 1999b], is updated for application at colder temperatures. The updated EQUISOLV II will be compared against AIM2 and APCM. The important equilibrium equations to solve in EQUISOLV II for the $NH_3/H_2SO_4/HNO_3/H_2O$ system are

$$HSO^-_{4(aq)} \overset{K_{HSO_4^-}}{\Longleftrightarrow} H^+_{(aq)} + SO^{2-}_{4(aq)}, \quad (11)$$

$$HNO_{3(g)} \overset{K_{HNO_3}}{\Longleftrightarrow} H^+_{(aq)} + NO^-_{3(aq)}, \quad (12)$$

Table 6. Mean Binary Activity Coefficients[a]

	$\alpha_k(T) = \beta_0 + \beta_1 T + \beta_2 T^2$		
Coefficients	β_0	β_1	β_2
		$HNO_3(n{=}5)$	
α_0	1.1550607531e+01	−8.6598065340e−02	1.6100335132e−04
α_1	−2.6045646534e+01	1.8570118152e−01	−3.4032931641e−04
α_2	9.6192566768e+00	−6.4314120728e−02	1.1363959743e−04
α_3	−1.4330104905e+00	9.3470490393e−03	−1.6321073928e−05
α_4	9.5181767818e−02	−6.1140131174e−04	1.0605856919e−06
α_5	−2.3568483179e−03	1.4936021604e−05	−2.5755879088e−08
		$(NH_4)_2SO_4(n{=}3)$	
α_0	3.4428316946e+00	−4.5328321654e−02	1.0202137529e−04
α_1	−1.0030630804e+00	6.0339372495e−03	−1.2162329645e−05
α_2	4.2925175339e−02	−3.0262230896e−04	5.9904176768e−07
α_3	−6.6813265363e−04	5.0031688798e−06	−9.7460258587e−09
		$NH_4NO_3(n{=}4)$	
α_0	2.7037375056e+00	−1.7880171498e−02	2.8497778393e−05
α_1	−4.9424685844e+00	2.1621849334e−02	−2.2789057453e−05
α_2	9.0584578176e−01	−4.2947161383e−03	4.7971905516e−06
α_3	−7.7554691781e−02	3.7618465057e−04	−4.3345626096e−07
α_4	2.4783745998e−03	−1.2123165585e−05	1.4181424491e−08
		$NH_4HSO_4(n{=}5)$	
α_0	9.9601477451e−01	−1.1296951291e−02	1.7452716744e−05
α_1	1.4845831451e+00	−9.3756384679e−03	1.8989492030e−05
α_2	−2.9273249432e−01	1.3469653174e−03	−2.2718917359e−06
α_3	2.1988585949e−02	−8.1477260064e−05	1.0470356871e−07
α_4	−7.5397112432e−04	2.2096863963e−06	−1.6051821078e−09
α_5	9.7902066682e−06	−2.1560396221e−08	−3.3248336670e−12

[a] $\ln\gamma = \sum_{k=0}^{n} \alpha_k(T) m^{k/2}$, Read 1.1550607531e+01 as 1.1550607531×10^1. All parameterizations are valid for 190^o K $\leq$ T $\leq$ 260^o K only. Ion activity for the H_2SO_4/H_2O system was not parameterized but instead tabulated in the computer codes.

$$NH_{3(g)} + H^+_{(aq)} \overset{K_{NH_3}}{\Longleftrightarrow} NH^+_{4(aq)}, \qquad (13)$$

where K_i is the equilibrium constant and (g) and (aq) refer to gas- and aqueous-phase species, respectively. The first dissociation step of H_2SO_4 ($H_2SO_{4(l)} \longrightarrow HSO^-_{4(aq)} + H^+_{(aq)}$) is assumed to be complete.

Temperature-dependent water and solute activity coefficients in EQUISOLV II are modified at cold temperatures (190°K-260°K) by parameterizing data from the model of *Clegg et al.* [1998a]. The temperature-dependent water activities of five electrolytes involved in equations (11)-(13), (H_2SO_4, HNO_3, $(NH_4)_2SO_4$, NH_4NO_3, NH_4HSO_4) are improved in EQUISOLV II. For consistency with previous work by *Tabazadeh et al.* [1997a, 1997b] the binary solution compositions are parameterized into

$$m = y_1(a_w) + \frac{(T - 190)\,[y_2(a_w) - y_1(a_w)]}{70}, \qquad (14)$$

where m is the molality of the binary electrolytes, a_w is the water activity (relative humidity expressed as fraction), and y is a function of a_w only (see Table 5). Mean binary activity coefficients (γ^o_{ij}) were parameterized by converting mole fraction activity coefficients (f) of *Clegg et al.*'s [1998a] model into molality base (γ) values according to equation (15), and using $\gamma^o_{ij} = \left(\gamma_i^{\nu_+}\gamma_j^{\nu_-}\right)^{\frac{1}{\nu_+ + \nu_-}}$ [*Pitzer*, 1991]:

$$f_i = \gamma_i \left(1 + \frac{M_w}{1000} \sum_k m_k\right), \qquad (15)$$

where ν_+ and ν_- are the stoichiometric coefficients of the binary electrolytes (for example, $\nu_+ = 2$ and $\nu_- = 1$ for $(NH_4)_2SO_4$), M_w is the molecular weight of water, and summation is over all solute species. The mean activity coefficients were then fitted into simple polynomial functions (given in Table 6) of temperature and molality (where α_k and β_k are polynomial coefficients):

Table 7. Model Conditions[a]

Cases	$r = \frac{NH_3}{H_2SO_4}$	NH_3, ppt	H_2SO_4, ppt	HNO_3, ppt	H_2O, ppm	Illustration
			Stratospheric Simulation (P_{total}=50 mbar)			
Background	r = 0.0	0.0	500.0	10,000.0	5.0	Figure 1a and 1b
Volcanic	r = 0.0	0.0	20,000.0	10,000.0	5.0	Figure 2a and 2b
			Upper Tropospheric Simulation (P_{total}=200 mbar)			
Background	r = 0.0	0.0	100.0	100.0	5.0, 50.0, 500.0	Figure 3a
	r = 1.0	100.0	100.0	100.0	5.0, 50.0, 500.0	Figure 3b
	r = 2.0	200.0	100.0	100.0	5.0, 50.0, 500.0	Figure 3c
Polluted	r = 0.0	0.0	100.0	2,000.0	5.0, 50.0, 500.0	Figure 4a
	r = 1.0	100.0	100.0	2,000.0	5.0, 50.0, 500.0	Figure 4b
	r = 2.0	200.0	100.0	2,000.0	5.0, 50.0, 500.0	Figure 4c
			HNO_3 Uptake (P_{total}=200 mbar)			
Background	r = 0.0 – 2.0	0.0 – 200.0	100.0	100.0	5.0, 50.0, 500.0	Figure 5
	r = ∞	100.0	0.0	200.0	5.0, 50.0, 500.0	

[a] P_{total} is total atmospheric pressure, and the mixing ratios used are atmospheric observations [*Tabazadeh et al.*, 1998; *Laaksonen et al.*, 1997].

$$\ln\gamma_{ij}^{o} = \sum_{k=0}^{n} \alpha_k(T) m^{k/2}, \quad (16a)$$

$$\alpha_k(T) = \beta_0 + \beta_1 T + \beta_2 T^2. \quad (16b)$$

The above parameterizations induce relative errors of no more than a few percents for both water and solute activities. The largest errors occur at low molality regions where ion activities usually exhibit a com-

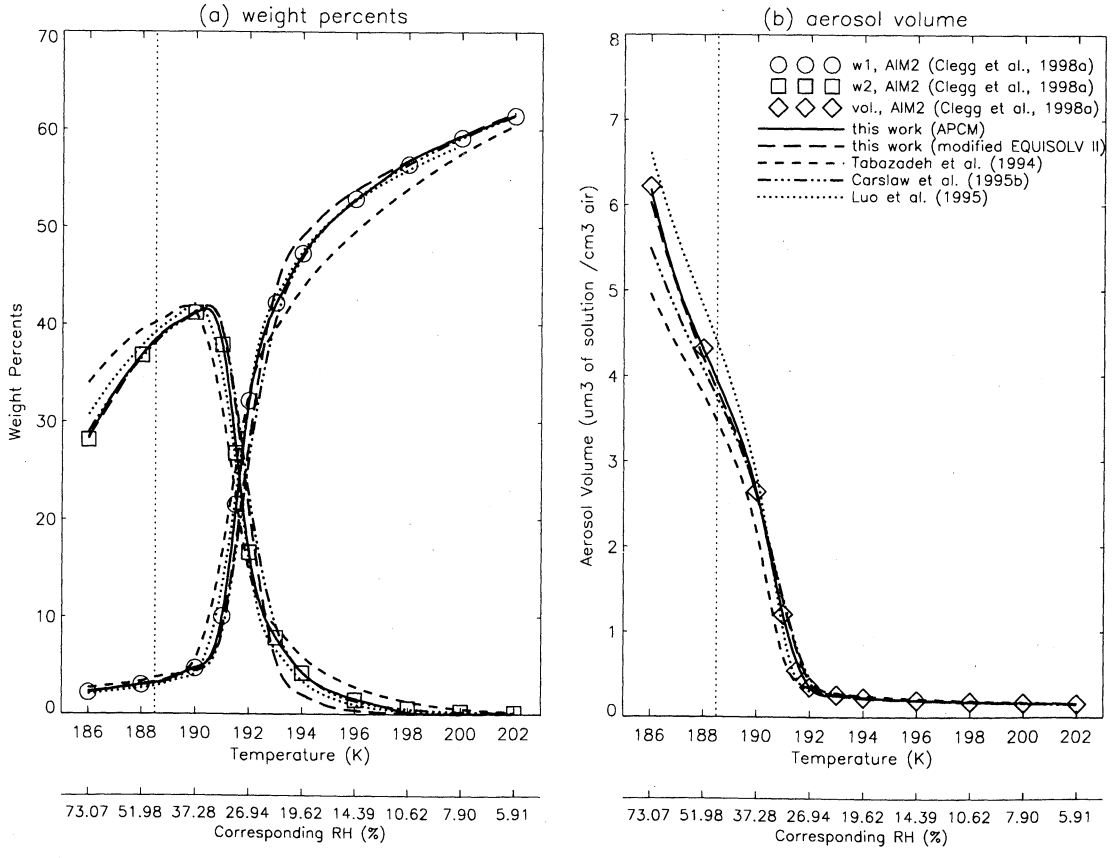

Figure 1. Comparison of various model predictions of (a) weight percents and (b) aerosol volume under background conditions in the stratosphere (see Table 7 for model conditions).

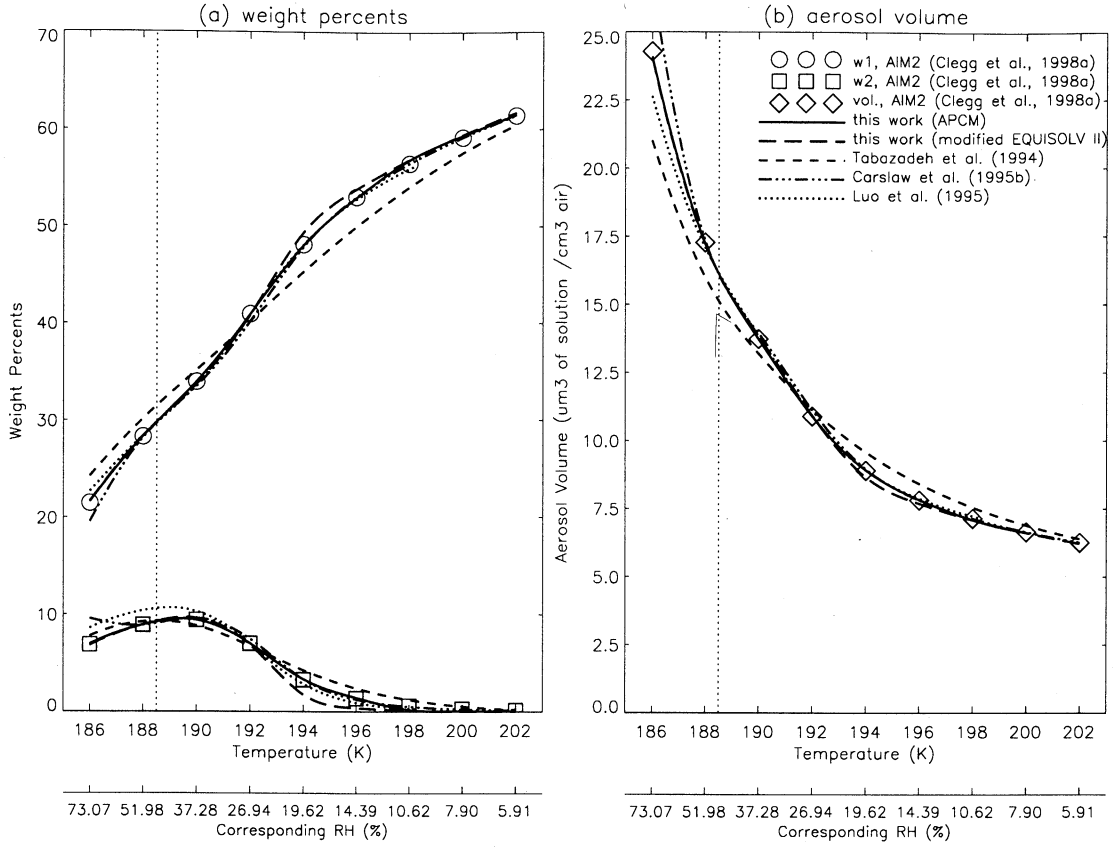

Figure 2. Comparison of various model predictions of (a) weight percents and (b) aerosol volume under volcanic conditions in the stratosphere (see Table 7 for model conditions).

plicated behavior. In addition to the improvement of binary water and solute activity coefficients, equilibrium constants of equations (11)-(13) were obtained from *Clegg et al.* [1998a] and converted into suitable molality-based units for use in EQUISOLV II. These modifications ensure perfect agreement of EQUISOLV II and AIM2 at a binary level where electrolyte solutions are made of H_2O plus only one electrolyte.

4. Model Intercomparison and Evaluation

4.1. $H_2SO_4/HNO_3/H_2O$

For the stratospheric system of $H_2SO_4/HNO_3/H_2O$, the compositions obtained from APCM are compared with previous formulations [*Carslaw et al.*, 1995b; *Luo et al.*, 1995; *Tabazadeh et al.*, 1994] under background and volcanic states (see Table 7 for model conditions used). Results from model intercomparisons between six different ternary aerosol models are shown in Figures 1 and 2. For the background stratosphere, APCM with Diff correction terms included is in good agreement with AIM2 [*Carslaw et al.*, 1995a]. The predicted weight percents by APCM overlap with AIM2 almost exactly throughout the entire temperature range shown in Figure 1a, whereas previous models deviate from AIM2 either at the initial, in the middle, or at the final stage of aerosol growth (Figure 1b). Under volcanic conditions (H_2SO_4 increases from 0.5 to 20ppb), all models produce nearly identical results with only slight variations (Figures 2a and 2b).

4.2. $NH_3/H_2SO_4/HNO_3/H_2O$

In the upper troposphere, aerosol compositions are examined for both background and polluted states (see Table 7 for model conditions). Under polluted conditions, HNO_3 mixing ratios are elevated well beyond background values of 100ppt [*Laaksonen et al.*, 1997], mainly because of convective transport of polluted boundary layer air directly into the upper troposphere. Variations in the aerosol composition predicted by three models, APCM, modified EQUISOLV II (with the improved activity data), and AIM2 [*Clegg et al.*, 1998a], are illustrated in Figures 3 and 4. The points of ice saturation are marked as vertical dotted lines in Figures 3 and 4. For all cases studied and compared, APCM yields compositions that are in close agreement with AIM2. The modified EQUISOLV II with new activity data performs better in the regions where relative humidity (RH) is high. The deviations at lower relative humidity are likely caused by the uncertainties in mixed activity coefficients calculated from simple mix-

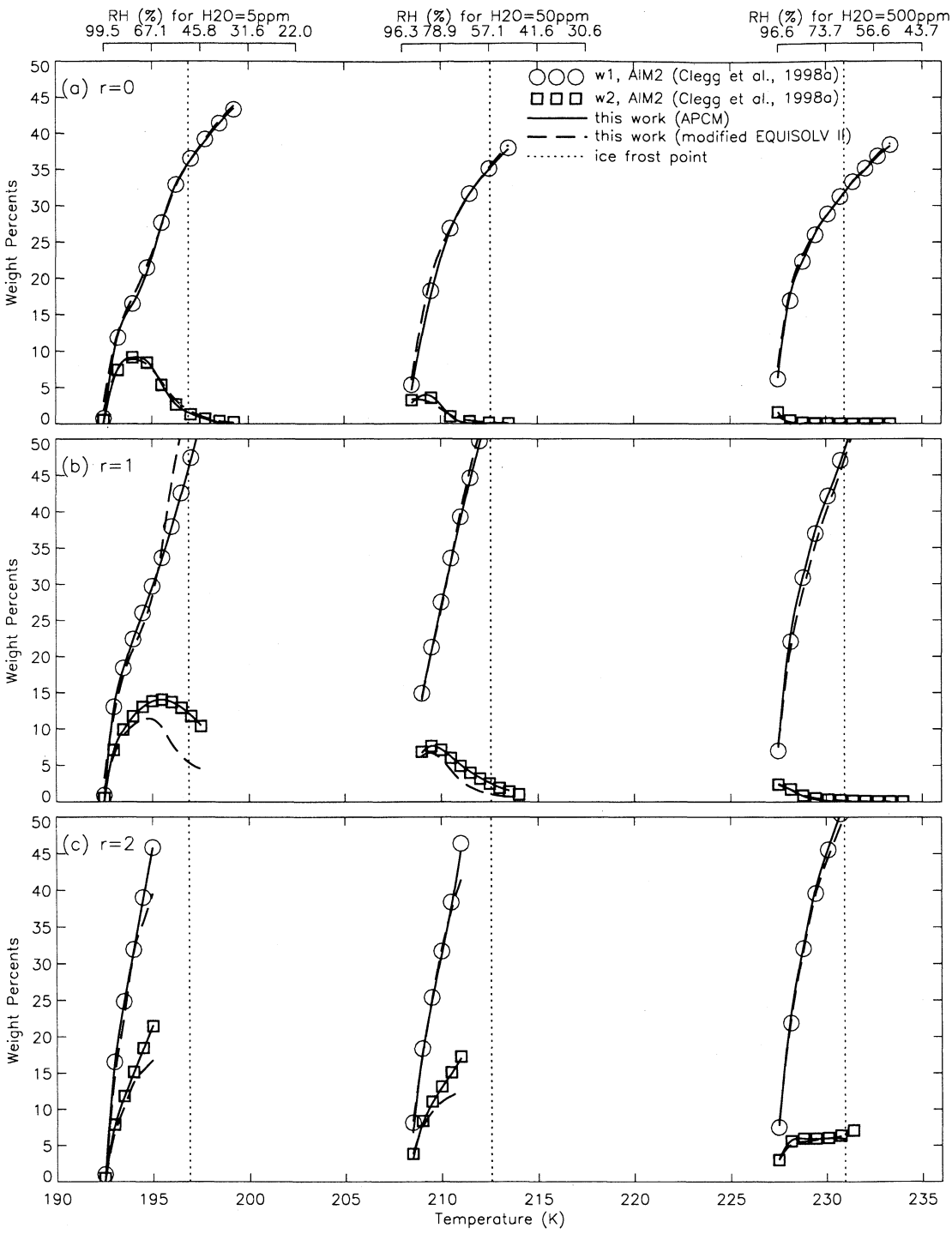

Figure 3. Variation of aerosol compositions as a function of temperature (or relative humidity) under background conditions in the upper troposphere (see Table 7 for model conditions). (a) $r = 0.0$, (b) $r = 1.0$, and (c) $r = 2.0$.

ing rules [*Bromley*, 1973; *Kusik and Meissner*, 1978] in EQUISOLV II.

We have also compared predicted molalities of individual components, NH_4^+, H_2SO_4 (= $HSO_4^- + SO_4^{2-}$), and NO_3^-, in solution (instead of weight percents of w_1 and w_2) and found that the differences between APCM and AIM2 are no more than a few percent except at the very low or high solute concentration regions. In other words, predictions by APCM are less accurate only in regions where weight percents approach the lower or upper limits (1% and 85%). Nevertheless, for very low weight percents, concentrations are too dilute to be significant, whereas for very high weight percents, relative humidities are sufficiently low that ammoniated salts, such as $(NH_4)_2SO_4$ or $(NH_4)_3H(SO_4)_2$ (letovicite), would most likely precipitate in solution

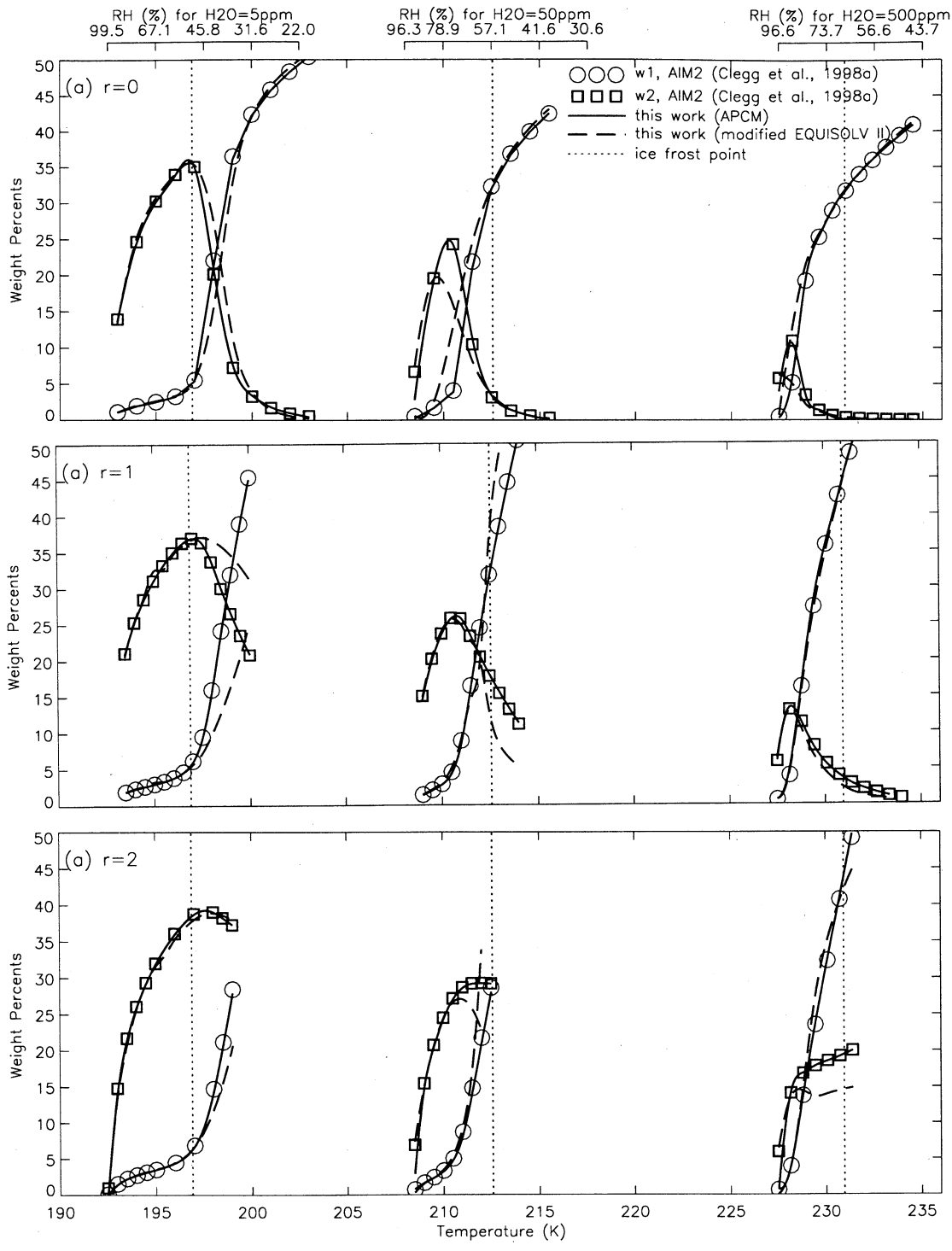

Figure 4. Variation of aerosol compositions as a function of temperature (or relative humidity) under polluted conditions in the upper troposphere (see Table 7 for model conditions). (a) $r = 0.0$, (b) $r = 1.0$, and (c) $r = 2.0$.

[*Tabazadeh and Toon*, 1998]. For example, crystallization of $(NH_4)_2SO_4$ occurs at $\sim 35\%$ RH at room temperature [*Xu et al.*, 1998]. At colder temperatures, crystallization of $(NH_4)_2SO_4$ will probably occur at slightly higher RHs. In addition, for very concentrated solutions ($w_1 + w_2 > 85\%$), aerosol compositions predicted by AIM2 are often outside the range of model validation [*Clegg et al.*, 1998a]. For the reasons mentioned above, the limits imposed on the weight percents in the APCM are not a serious drawback. Also, as shown in Figures 3 and 4, the APCM compositions are most accurate near regions where ice reaches saturation in the atmosphere.

In addition to aerosol composition the APCM can be used to calculate the extent of HNO_3 uptake by up-

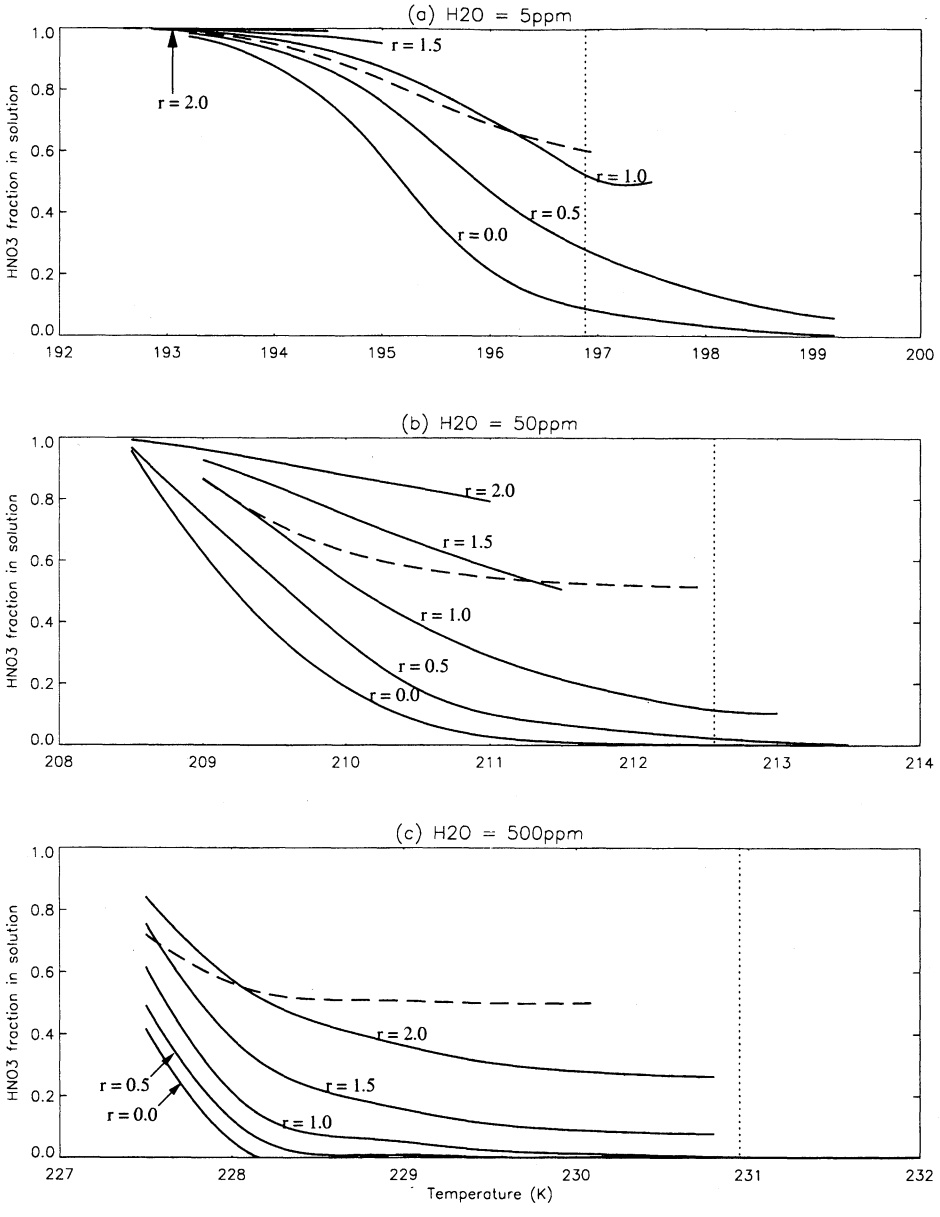

Figure 5. Uptake of HNO_3 in sulfate-based aerosols as a function of sulfate neutralization under background conditions in the upper troposphere (see Table 7 for model conditions). (a) H_2O = 5ppm, (b) H_2O = 50ppm, and (c) H_2O = 500ppm. (Dashed lines represent the uptake by pure NH_4NO_3 aerosols (i.e., H_2SO_4 = 0))

per tropospheric aerosols. Aircraft field experiments have shown that ammoniated particles are abundant in the upper troposphere [*Talbot et al.*, 1996, 1998; *Tabazadeh et al.*, 1998]. Here we examine how HNO_3 uptake may be affected by the presence of ammoniated aerosols in the upper troposphere. For simulations the H_2SO_4 and HNO_3 mixing ratios are fixed at background levels of 100 ppt each. NH_3 concentrations in the APCM are varied by increasing (or decreasing) r to account for changes in solution neutrality (or pH), ranging from pure H_2SO_4 solution droplets (r = 0.0) to fully ammoniated systems consisting of only $(NH_4)_2SO_4$ (r = 2.0) (see Table 7 for model conditions used).

In Figure 5, the uptake of HNO_3, expressed as a fraction (i.e., ratio of concentration in the liquid phase to the total initial concentration), is shown for three different assumed water vapor pressure profiles. As expected, partitioning of HNO_3 in sulfate-based aerosols depends strongly on solution neutrality. In general, greater uptake occurs at lower temperatures and higher relative humidities. For example, at temperatures lower than 210°K (which corresponds to a relative humidity of 78% for P_{total} = 200mb and H_2O = 50ppm), a significant fraction (> 90%) of HNO_3 resides in fully neutralized ammoniated solutions, compared to only < 20% in the pure sulfate system (Figure 5b). It has been shown that

high levels of HNO_3 in solution may cause precipitation of ammoniated and/or nitrated salts, which could change the mode of ice formation from homogeneous to heterogeneous nucleation [*Tabazadeh and Toon*, 1998].

5. Conclusions

The ion interaction model of *Clegg et al.* [1998a] for the system of $NH_3/H_2SO_4/HNO_3/H_2O$ has been parameterized into a compact model well suited for incorporation into large-scale atmospheric models. The aerosol physical chemistry model (APCM) reproduces the AIM2 results of *Clegg et al.* [1998a] for a wide range of conditions in the upper troposphere and lower stratosphere. Model intercomparisons show that for the ternary system of $H_2SO_4/HNO_3/H_2O$ solution compositions obtained from APCM are in better agreement with those obtained from AIM2 than previous formulations. For the quaternary system of $NH_3/H_2SO_4/HNO_3/H_2O$, APCM results are also in good agreement with AIM2 predictions, particularly near the regions of ice saturation where the influence of ammoniated particles on the ice nucleation process is of interest. Extension of APCM to include other features such as calculations of deliquescence relative humidity and precipitation of solids in solution are under way.

Acknowledgments. This work is supported by NASA Atmospheric Chemistry Modeling and Analysis Program. A.T. acknowledges support from a Presidential Early Career Award for Science and Engineers. We thank Simon Clegg for many helpful discussions and for providing us with a computer code of the mixed electrolyte system. The AIM2 results in this work were obtained by running the "comprehensive" version of model II available at http://www.uea.ac.uk/~e770/aim.html. We are also grateful to Mark Jacobson for a copy of the EQUISOLV II and many helpful discussions. For a computer copy of the aerosol code and lookup tables send e-mail to lin@ice.arc.nasa.gov.

References

Adams, P. J., J. H. Seinfeld, and D. M. Koch, Global concentrations of tropospheric sulfate, nitrate, and ammonium aerosol simulated in a general circulation model, *J. Geophys. Res.*, *104*, 13,791, 1999.

Bassett, M., and J. H. Seinfeld, Atmospheric equilibrium model of sulfate and nitrate aerosols, *Atmos. Environ.*, *17*, 2237, 1983.

Bromley, L. A., Thermodynamic properties of strong electrolytes in aqueous solutions, *AIChE J.*, *19*, 313, 1973.

Carslaw, K. S., B. P. Luo, S. L. Clegg, T. Peter, P. Brimblecombe, and P. Crutzen, Stratospheric aerosol growth and HNO_3 gas phase depletion from coupled HNO_3 and water uptake by liquid particles, *Geophys. Res. Lett.*, *21*, 2479, 1994.

Carslaw, K. S., S. L. Clegg, and P. Brimblecombe, A thermodynamic model of the system $HCl-HNO_3-H_2SO_4-H_2O$, including solubilities of HBr, from 328K to < 200K. *J. Phys. Chem.*, *99*, 11,557, 1995a.

Carslaw, K. S., B. P. Luo, and T. Peter, An analytic expression for the composition of aqueous $HNO_3-H_2SO_4$ stratospheric aerosols including gas phase removal of HNO_3, *Geophys. Res. Lett.*, *22*, 1877, 1995b.

Clegg., S. L., and P. Brimblecombe, Equilibrium partial pressures and mean activity and osmotic coefficients of $0-100\%$ nitric acid as a function of temperature, *J. Phys. Chem.*, *94*, 5369, 1990.

Clegg., S. L., and P. Brimblecombe, A generalized multicomponent thermodynamic model applied to the $(NH_4)_2SO_4-H_2SO_4-H_2O$ system to high supersaturation and low relative humidity at 298.15K, *J. Aerosol Sci.*, *26*, 19, 1995a.

Clegg., S. L., and P. Brimblecombe, Application of a multicomponent thermodynamic model to activities and thermal properties of $0-40$ mol kg^{-1} aqueous sulfuric acid from < 200 to 328K, *J. Chem. Eng. Data*, *40*, 43, 1995b.

Clegg, S. L., P. Brimblecombe, and A. S. Wexler, A thermodynamic model of the system $H^+-NH_4^+-O_4^{-2}-NO_3^--H_2O$ at tropospheric temperatures, *J. Phys. Chem. A*, *102*, 2137, 1998a.

Clegg, S. L., P. Brimblecombe, and A. S. Wexler, A thermodynamic model of the system $H^+-NH_4^+-Na^+-SO_4^{-2}-NO_3^--Cl^--H_2O$ at 298.15K, *J. Phys. Chem. A*, *102*, 2155, 1998b.

Jacobson, M. Z., *Fundamentals of Atmospheric Modeling*, Cambridge Univ. Press, New York, 1999a.

Jacobson, M. Z., Studying the effects of calcium and magnesium on size-distributed nitrate and ammonium with EQUISOLV II, *Atmos. Environ.*, *33*, 3635, 1999b.

Jacobson, M. Z., A physically-based treatment of elemental carbon optics: Implications for global direct forcing of aerosols, *Geophys. Res. Lett.*, *27*, 217, 2000.

Jacobson, M. Z., A. Tabazadeh, and R. P. Turco, Simulating equilibrium within aerosols and nonequilibrium between gases and aerosols, *J. Geophys. Res.*, *101*, 9079, 1996.

Kärcher, B., and S. Solomon, On the composition and optical extinction of particles in the tropopause region, *J. Geophys. Res.*, 104, 27,441, 1999.

Kim, Y. P., and J. H. Seinfeld, Atmospheric gas-aerosol equilibrium, III, Thermodynamics of crustal elements Ca^{2+}, K^+, and Mg^{2+}, *Aerosol Sci. Technol.*, *22*, 93, 1995.

Kusik, C. L., and H. P. Meissner, Electrolyte activity coefficients in inorganic processing, *AIChE Symp. Ser.*, *74*, 14, 1978.

Laaksonen, A., J. Hienola, and M. Kulmala, Supercooled cirrus cloud formation modified by nitric acid pollution of the upper troposphere, *Geophys. Res. Lett.*, *24*, 3009, 1997.

Luo, B., K. S. Carslaw, T. Peter, and S. L. Clegg, Vapor pressures of $H_2SO_4/HNO_3/HCl/HBr/H_2O$ solutions to low stratospheric temperatures, *Geophys. Res. Lett.*, *22*, 247, 1995.

Pilinis, C., and J. H. Seinfeld, Continued development of a general equilibrium model for inorganic multicomponent atmospheric aerosols, *Atmos. Environ.*, *32*, 2453, 1987.

Pitzer, K. S., *Activity Coefficients in Electrolyte Solutions*, 2nd ed., CRC Press, Boca Raton, Fla., 1991.

Saxena, P., C. Seigneur, A. B. Hudischewskyj, and J. H. Seinfeld, A comparative study of equilibrium approaches to the chemical characterizations of secondary aerosols, *Atmos. Environ.*, *20*, 1471, 1986.

Solomon, S., Stratospheric ozone depletion: A review of concepts and history, *Rev. Geophys.*, *37*, 275, 1999.

Stelson, A. W., and J. H. Seinfeld, Relative humidity and temperature dependence of the ammonium nitrate dissociation constant, *Atmos. Environ.*, *26*, 983, 1981.

Stokes, R. H., and R. A. Robinson, Interactions in aqueous nonelectrolyte solutions, **I**, solute-solvent equilibria, *J. Phys. Chem.*, *70*, 2126, 1966.

Tabazadeh, A., and O. B. Toon, The role of ammoniated aerosols in cirrus cloud nucleation, *Geophys. Res. Lett.*, *25*, 1379, 1998.

Tabazadeh, A., R. P. Turco, and M. Z. Jacobson, A model for studying the composition and chemical effects of stratospheric aerosols, *J. Geophys. Res.*, *99*, 12,897, 1994.

Tabazadeh, A., O. B. Toon, S. Clegg, and P. Hamill, A new parameterization of H_2SO_4/H_2O aerosol composition: Atmospheric implications, *Geophys. Res. Lett.*, *24*, 1931, 1997a.

Tabazadeh, A., O. B. Toon, and E. Jensen, Formation and implications of ice particle nucleation in the stratosphere, *Geophys. Res. Lett.*, *24*, 2007, 1997b.

Tabazadeh, A., M. Z. Jacobson, H. B. Singh, O. B. Toon, J. S. Lin, B. Chatfield, A. N. Thakur, R. W. Talbot, and J. E. Dibb, Nitric acid scavenging by mineral and biomass aerosols, *Geophys. Res. Lett.*, *25*, 4185, 1998.

Talbot, R. W. et al., Chemical characteristics of continental outflow from Asia to the troposphere over the western Pacific Ocean during September-October 1991: Results from PEM-West A, *J. Geophys. Res.*, *101*, 1713, 1996.

Talbot, R. W., J. E. Dibb, and M. B. Loomis, Influence of vertical transport on free tropospheric aerosols over the central USA in springtime, *Geophys. Res. Lett.*, *25*, 1367, 1998.

Weisenstein, D. K., Y. K. Glenn, M. K. W. Ko, N. Sze, J. M. Rodriguez, and C. J. Scott, A two-dimensional model of sulfur species and aerosols, *J. Geophys. Res.*, *102*, 13,019, 1997.

Wexler, A. S., and J. H. Seinfeld, Second–generation inorganic aerosol model, *Atmos. Environ., Part A*, 25, 2731, 1991.

Xu, J., D. Imre, R. McGraw, and I. Tang, Ammonium sulfate: Equilibrium and metastability phase diagrams from 40°C to −50°C, *J. Phys. Chem. B*, *102*, 7462, 1998.

J. S. Lin and A. Tabazadeh, NASA Ames Research Center, MS 245-4, Moffett Field, CA 94035. (lin@ice.arc.nasa.gov; atabazadeh@mail.arc.nasa.gov)

(Received May 11, 2000; revised August 29, 2000; accepted September 15, 2000.)